

The structure of the amorphous phase as the basis for the rapid change in DVD materials

S. Kohara^{1,2*}, Y. Tanaka^{2,3}, Y. Fukuyama^{1,2}, N. Yasuda^{1,2}, J. Kim^{1,2}, H. Murayama⁴, S. Kimura^{1,2}, K. Kato^{2,3}, Y. Moritomo^{2,5}, T. Matsunaga^{2,6}, R. Kojima^{2,6}, N. Yamada^{2,6}, H. Tanaka⁷, T. Ohshima⁷, J. Akola^{8,9}, R. O. Jones⁹
and M. Takata^{1,2,3,10}

¹JASRI/ SPring-8, 1-1-1 Kouto, Sayo-cho, Sayo-gun, Hyogo 679-5198, Japan

²JST, CREST, 5 Sanbancho, Chiyoda-ku, Tokyo 102-0075, Japan

³RIKEN SPring-8 Center, 1-1-1 Kouto, Sayo-cho, Sayo-gun, Hyogo 679-5148, Japan

⁴Applied Chemistry, Science and Engineering, Chuo University, 1-13-27 Kasuga, Tokyo 112-8551, Japan

⁵The Graduate School of Pure and Applied Sciences, University of Tsukuba, Tennodai, Tsukuba, Ibaraki 305-8571, Japan

⁶Panasonic Corporation, 3-1-1 Yagumo-Nakamachi, Moriguchi, Osaka 570-8501, Japan

⁷XFEL Project Head Office/RIKEN, 1-1-1 Kouto, Sayo-cho, Sayo-gun, Hyogo 679-5148, Japan

⁸Nanoscience Center, Department of Physics, P.O. Box 35, FI-40014 University of Jyväskylä, Finland

⁹Institut für Festkörperforschung, Forschungszentrum Jülich, D-52425 Jülich, Germany

¹⁰Department of Advanced Materials Science, School of Frontier Science, The University of Tokyo, 5-1-5, Kashiwanoha, Chiba 277-8561, Japan

*E-mail address: kohara@spring8.or.jp

ABSTRACT

We have determined the structure of amorphous $\text{Ge}_2\text{Sb}_2\text{Te}_5$ by combining DFT/MD simulations and reverse Monte Carlo techniques to obtain a structural model that reproduces both x-ray diffraction and x-ray photoelectron spectroscopy data. There are many 4-fold rings in the atomic configuration of the amorphous phase, and we suggest that these rings can be nuclei for crystallization. Furthermore, time-resolved x-ray diffraction measurements combined with photorefectivity measurements on the crystallization process of the amorphous phase suggest that the crystallization process of $\text{Ge}_2\text{Sb}_2\text{Te}_5$ can be explained by a nucleation-driven process. We propose that the presence of many 4-fold rings is the reason for the rapid crystallization in $\text{Ge}_2\text{Sb}_2\text{Te}_5$ with a nucleation-driven process.

Key words: Phase-change materials, $\text{Ge}_2\text{Sb}_2\text{Te}_5$, Time-resolved x-ray diffraction, DFT/MD simulation

1. INTRODUCTION

Phase-change materials, which utilize the melt-quenching (amorphization for record) and annealing (crystallization for erase) processes of chalcogenide materials, are essential to the development of information technologies. The application of reversible amorphous–crystal phase changes for memory devices was proposed by Ovshinsky in the 1960's, where a memory switch can be generated on the basis of changes in the electrical properties of these phases in chalcogenide materials.¹⁾ The development of Ge-Sb-Te²⁾ system and Ag-In-Sb-Te³⁾ system has allowed the development and production of rewritable compact discs (CDs), DVDs, and Blu-ray discs. Phase-change materials are now well-established media, but the rapid phase-change mechanism and the 3-dimensional atomic configuration in the amorphous phase are still unclear.

Structure of amorphous $\text{Ge}_2\text{Sb}_2\text{Te}_5$ (*a*- $\text{Ge}_2\text{Sb}_2\text{Te}_5$) has been widely studied by diffraction,⁴⁻⁷⁾ spectroscopy,⁸⁻¹⁰⁾ and theoretical simulations,¹¹⁻¹⁶⁾ particularly after the landmark study of Kolobov *et al.*,⁸⁾ but the details of the structure remain controversial. We have studied the structure of *a*- $\text{Ge}_2\text{Sb}_2\text{Te}_5$ by a combination of high-energy x-ray diffraction, reverse Monte Carlo (RMC) modelling,⁶⁾ and DFT/MD simulation¹⁴⁾ and found large fractions of 4-fold and 6-fold rings in the atomic configuration. The bond angle distributions exhibit a peak at approximately 90°, corresponding to that in the crystal phase. Furthermore, we have combined time-resolved x-ray diffraction measurement with photorefectivity measurement and found that $\text{Ge}_2\text{Sb}_2\text{Te}_5$ exhibits a three-stage crystallization process,¹⁷⁾ which

$\text{Ag}_{3.5}\text{In}_{3.8}\text{Sb}_{75.0}\text{Te}_{17.7}$ does not show.¹⁸⁾ Here we compare the structure of $\alpha\text{-Ge}_2\text{Sb}_2\text{Te}_5$ obtained by RMC modelling and density-functional theory (DFT) / molecular dynamics (MD) simulation and refine the structure to reproduce both x-ray diffraction and x-ray photoelectron spectroscopy (XPS) data.¹⁹⁾ The structural origin of the rapid crystallization process in $\text{Ge}_2\text{Sb}_2\text{Te}_5$ is discussed on the basis of the amorphous structure and crystallization behavior.

2. EXPERIMENTS

2.1 Sample preparation

The specimen for high-energy x-ray diffraction experiments were made by laminating an organic film sheet on a glass disc with a diameter of 120 mm and sputtering to form the recording film with a thickness of 200 - 500 nm. The organic film was scratched from the glass disc, and the specimen was removed from the glass substrate using a spatula. The composition of the sample was examined by inductively coupled plasma atomic emission spectrometry. The 300-nm thick samples for time-resolved x-ray diffraction experiments were prepared by depositing $\text{Ge}_2\text{Sb}_2\text{Te}_5$ on a SiO_2 glass substrate (12 cm diameter and 0.6 mm thick) with a 2-nm thick 80 mol% ZnS–20 mol% SiO_2 cap layer.

2.2 High-energy x-ray diffraction experiment

The high-energy x-ray diffraction experiments were carried out at the high-energy x-ray diffraction beamline BL04B2²⁰⁾. The diffraction patterns of powder sample in a thin walled (10 μm) tube of 1 mm diameter (supplier: GLAS Müller, D-13503 Berlin) and an empty tube were measured in a transmission geometry. The collected data were corrected using standard programs,²⁰⁾ and these data were normalized to give the total structure factor $S(Q)$.

2.3 Time-resolved x-ray diffraction experiment

The time-resolved x-ray diffraction measurements were performed on $\alpha\text{-Ge}_2\text{Sb}_2\text{Te}_5$ at the BL40XU beamline,²¹⁾ in order to reveal the crystallization process of the amorphous phase. We measured (i) the time constants of both crystallization and optical reflectivity changes, and (ii) the crystallization behavior. We employed avalanche photodiode (APD)/multi-channel scaling (MCS) measurements, with a time resolution of 3.2 ns, coupled with photorefectivity measurement for (i) and imaging plate (IP)/pump–probe measurement of a time resolution of 40 ps for (ii). The details of the time-resolved measurement are given in ref. 18.

2.4 DFT/MD simulation and structure refinement by RMC modelling

The DFT/MD calculations were performed with the CPMD package.²²⁾ In this study we use for the exchange-correlation energy the approximation of Tao *et al.* (TPSS),²³⁾ which was developed to improve results obtained with generalized gradient approximations. The initial structure was based on that of crystalline $\text{Ge}_2\text{Sb}_2\text{Te}_5$ (NaCl-type structure) with 460 atoms and 52 vacancies, and the starting temperature was 3000 K. The long simulation time (300 ps) is essential for a realistic description of the number of “wrong bonds” (*i.e.*, bonds that do not occur in the crystalline phase), whose number decreases steadily as the temperature is lowered.

Structural refinements by RMC modelling were carried out using the RMC++ code,²⁴⁾ which allows us to apply bond angle constraints. The DFT/MD optimized configuration was used as an initial configuration in the RMC refinement. A cutoff distance of 3.2 Å is used to analyze bond angles and ring distributions.

3. RESULTS & DISCUSSION

3.1 The refined structure of α -Ge₂Sb₂Te₅ obtained by a combination of DFT/MD simulation and RMC modelling

First, we calculated the total pair distribution function $g(r)$ from the DFT/MD model¹⁴⁾ and x-ray photoelectron spectroscopy (XPS) valence-band spectrum from the RMC model,⁶⁾ which were not calculated in our initial study.¹⁷⁾ The total structure factor $S(Q)$ and pair distribution function $g(r)$ obtained by high-energy x-ray diffraction (HEXRD) experiment⁶⁾ are shown in Fig. 1, together with the results of DFT/MD simulation. The $S(Q)$ calculated from the DFT/MD simulation shows relatively good agreement with the experimental data due to the use of a large simulation box. However, the bond length of the first correlation peak in $g(r)$ calculated from the DFT/MD simulation is much greater than in the experiment. In particular, the partial pair distributions $g_{ij}(r)$ calculated from the DFT/MD model suggest that the Ge-Te correlation length in the DFT/MD model is longer than the experimental value. The experimental XPS valence-band spectrum¹⁰⁾ and the spectrum calculated from the RMC model are shown in Fig. 2. It is obvious that the RMC model does not show a band gap in the spectrum, suggesting that the RMC optimized configuration does not describe the electronic structure in the amorphous phase correctly.

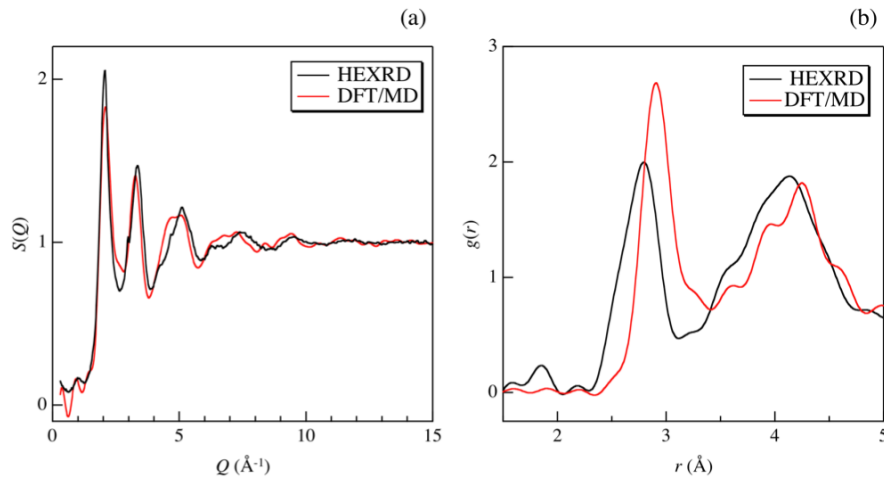


Fig. 1. Total structure factor $S(Q)$ (a) and pair distribution function $g(r)$ (b) of the DFT/MD model for α -Ge₂Sb₂Te₅.

Since we had found problems with both the RMC and DFT/MD models, we refined the structure by combining RMC modelling and DFT/MD simulations. The RMC refinement was carried out using the x-ray $S(Q)$ and the DFT/MD optimized configuration as the initial configuration, with the maximum movement for any atom at each MC step of 0.14 \AA . After a one minute RMC simulation, the agreement between experimental data and the refined RMC-DFT/MD model was excellent. However, the XPS valence-band spectrum calculated from the refined structure did not show a band gap. To clarify the structural difference between the DFT/MD model and RMC-DFT/MD model, we show the bond angle distributions of Te-Ge-Te and Te-Sb-Te in Fig. 3. Both the DFT/MD model (initial configuration for the RMC modelling) and the RMC refined model exhibit a peak at approximately 90° , but the peak is very broad and has a tail to the large angle region in the refined RMC-DFT/MD model. Such a feature can be seen in the result of another RMC study using two

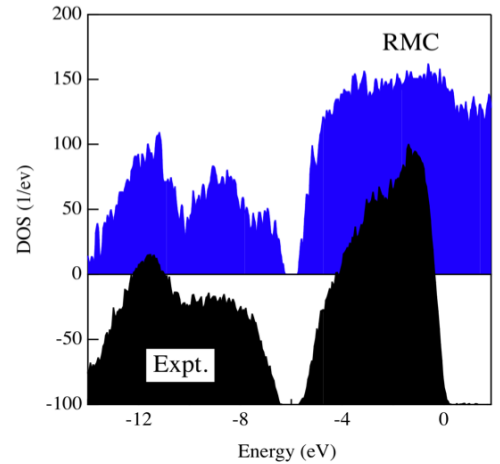


Fig. 2. XPS valence-band spectrum of the RMC model for α -Ge₂Sb₂Te₅. Experimental data are displaced downward for clarity.

diffraction and three EXAFS data sets,⁷⁾ because RMC can find structures that are consistent with experimental data on most disordered systems.²⁵⁾

To overcome this problem, the bond angle distributions were constrained in the RMC refinement. The total structure factor $S(Q)$ and pair distribution function $g(r)$ calculated from the refined RMC model are shown in Fig. 4. As can be seen in Fig. 4(a), the agreement between the experimental data and the RMC-DFT/MD is excellent up to maximum Q value of 20 \AA^{-1} . The $g(r)$ calculated from the refined RMC-DFT/MD model also shows good agreement with experimental data. Figure 5 shows the experimental XPS valence-band spectrum and the spectrum calculated from the RMC-DFT/MD model. Our final refined model has a band gap and agrees well with the experimental data. The ring statistics calculated up to 12-fold rings of the refined RMC-DFT/MD model are shown in Fig. 6. The final structure shows a significant number of 4-fold rings with $ABAB$ alternation (A : Ge, Sb; B : Te).

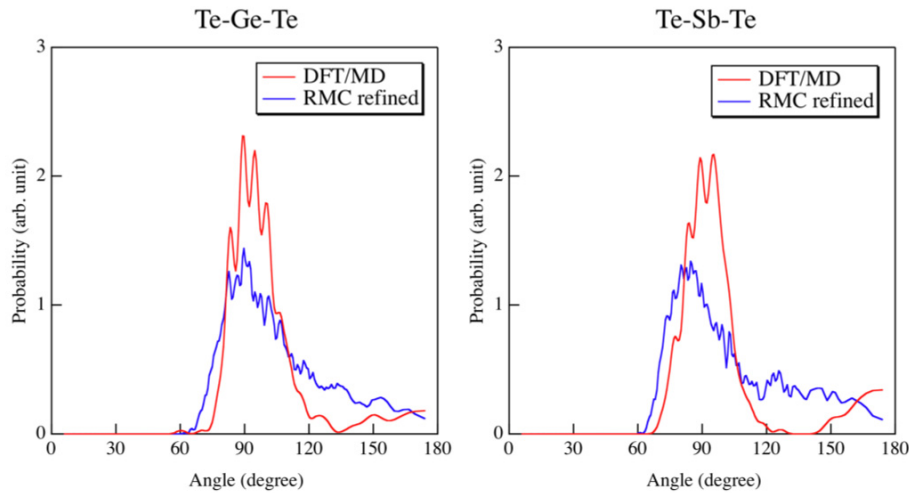


Fig. 3. Bond angle distribution of $a\text{-Ge}_2\text{Sb}_2\text{Te}_5$.

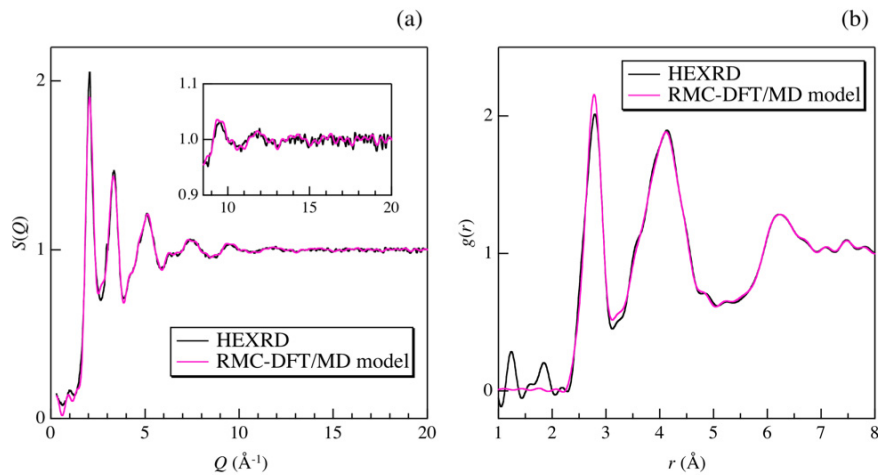


Fig. 4. Total structure factor $S(Q)$ (a) and pair distribution function $g(r)$ (b) of the RMC-DFT/MD model for $a\text{-Ge}_2\text{Sb}_2\text{Te}_5$.

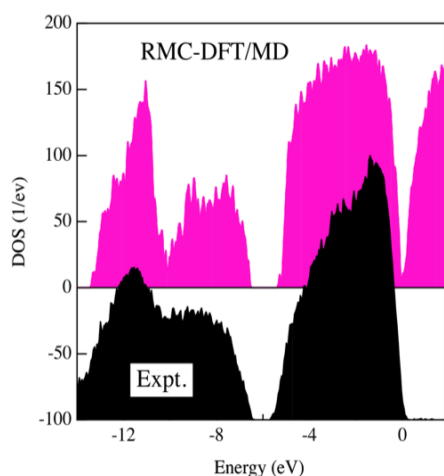


Fig. 5. XPS valence-band spectrum of the RMC-DFT/MD model for $a\text{-Ge}_2\text{Sb}_2\text{Te}_5$. Experimental data are displaced downward for clarity.

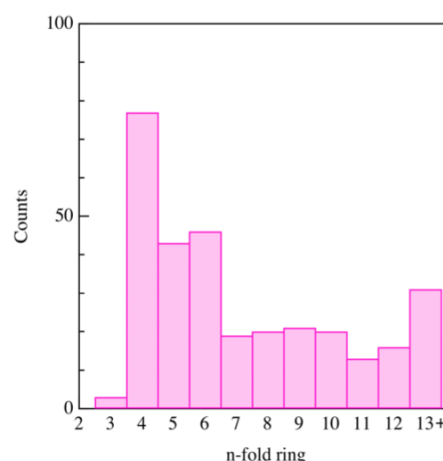


Fig. 6. Ring statistics of the RMC-DFT/MD model for $a\text{-Ge}_2\text{Sb}_2\text{Te}_5$.

3.2 Time-resolved x-ray diffraction experiment and the mechanism of the rapid phase change

To investigate the crystallization behavior of $a\text{-Ge}_2\text{Sb}_2\text{Te}_5$, we have studied the time-evolution of x-ray diffraction pattern combined with photoreflectivity measurements on $\text{Ge}_2\text{Sb}_2\text{Te}_5$.¹⁸⁾ The time-resolved x-ray diffraction pattern and photoreflectivity profile of 300-nm-thick $\text{Ge}_2\text{Sb}_2\text{Te}_5$ sample are shown in Fig. 7. Both profiles exhibit a rapid increase in the photoreflectivity between 100 and 200 ns. Wei and Gan reported the change in photoreflectivity of a 30 nm-thick $\text{Ge}_2\text{Sb}_2\text{Te}_5$ film deposited by dc-magnetron sputtering and found three stages for the crystallization: an onset stage (~ 40 ns), a nucleation stage (~ 120 ns), and a growth stage (~ 140 ns).¹⁷⁾ These stages can be observed in the photoreflectivity profile of $\text{Ge}_2\text{Sb}_2\text{Te}_5$; an onset stage of ~ 100 ns, a nucleation stage of ~ 200 ns and a growth stage, as indicated by arrows.

To obtain more information about the phase-change process, we have analyzed the time resolved x-ray diffraction profiles (Fig. 7). As can be seen there, the x-ray diffraction intensity profiles of all Bragg peaks are consistent with the photoreflectivity profiles. To estimate the time constant, the x-ray diffraction data of 200 Bragg peak were fitted by a linear function, and the times which the function exhibits 0 and 100 % of diffraction intensity change were defined as “start” and “end”, respectively: the start and the end times are 90 (1) and 273 (1) ns, respectively. The diffraction intensity increases and saturates at approximately 300 ns, indicating that crystallization of $a\text{-Ge}_2\text{Sb}_2\text{Te}_5$ is almost complete within

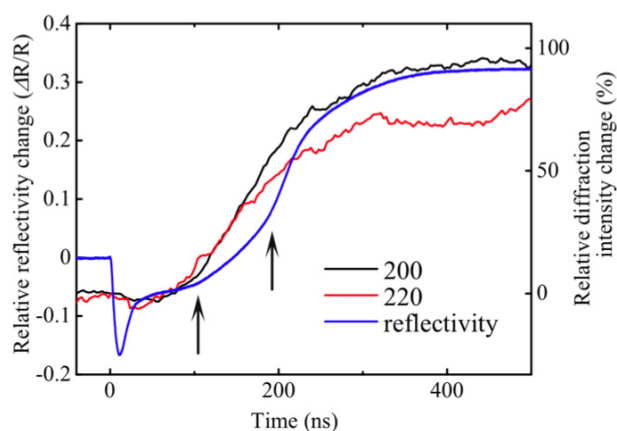


Fig. 7. Photoreflectivity and time resolved x-ray diffraction profiles of $\text{Ge}_2\text{Sb}_2\text{Te}_5$ obtained by APD/MCS measurement. Photoreflectivity profiles were measured from the right and rear sides of the discs. The profile from the rear side is almost the same as that of the right side except for a negative peak at approximately 20 ns. The changes in relative diffraction intensity were normalized by the intensity at $5\ \mu\text{s}$. The grey arrows indicate the boundary of the three stages discussed in Ref. 17.

that time. Consequently, although the thickness of the sample in our study is greater than that in commercially available devices, our results are evidence of a strong relationship between x-ray diffraction intensity and the photorefectivity of the phase-change materials, *i.e.*, the structure and the electronic properties.

From the intensity profile measured by the APD/MCS method, the delay times τ were determined for the IP/pump-probe method, and figure 8(a) shows the diffraction patterns obtained for a 40 ps snapshot using this method. Since the intensity of each diffraction peak increases uniformly with time, there is no crystal-crystal phase transition during the crystal growth. However, the positions of the diffraction peaks shift to a higher angle, corresponding to a lattice parameter shrinkage of about 1 %, due to the time-dependent temperature decrease. Furthermore, the peak width for the 200 reflection is almost constant during crystallization, as shown in Fig. 8(b), indicating that the grain sizes do not change after 100 ns.

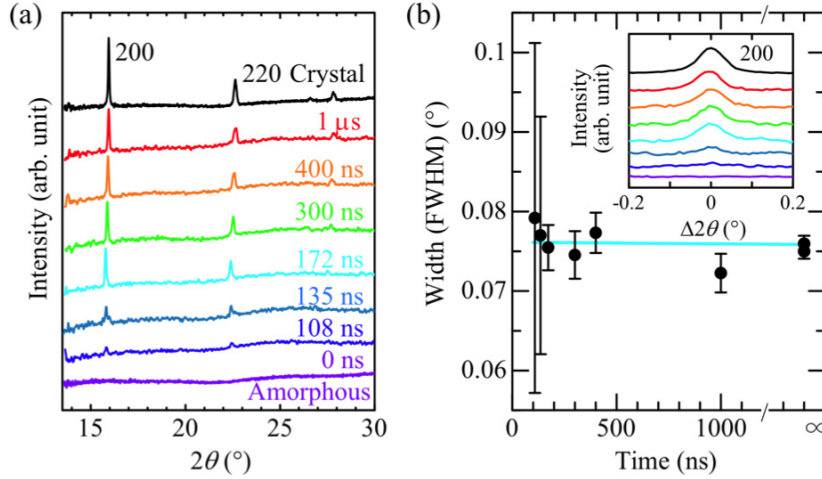


Fig. 8. (a) Time dependent x-ray diffraction patterns of $\text{Ge}_2\text{Sb}_2\text{Te}_5$ obtained by the IP/pump-probe method. (b) Changes in peak width for the 200 reflection of $\text{Ge}_2\text{Sb}_2\text{Te}_5$. The inset shows close-ups of the 200 reflection peaks. The positions of the Bragg peaks calculated by curve fitting were offset to zero for clarity.

From the above experimental findings, we propose the following model for crystallization in $\text{Ge}_2\text{Sb}_2\text{Te}_5$. Nucleation takes place in the whole area in the amorphous phase after laser irradiation, and the number of newly formed crystallites increases during the cooling process until 300 ns. The crystal growth is then disturbed when the crystallites impinge on each other. This model is consistent with the nucleation-driven crystallization process discussed in ref. 26. Furthermore, we stress that the large number of 4-fold ring found show *ABAB* alternation (*A*: Ge, Sb; *B*: Te) in the amorphous structure obtained by RMC-DFT/MD simulation. These units are also present in the NaCl lattice of the crystalline phase and can be viewed as essential for rapid crystallization.

4. CONCLUSION

We have performed synchrotron x-ray diffraction experiment on amorphous $\text{Ge}_2\text{Sb}_2\text{Te}_5$ and a time-resolved synchrotron x-ray diffraction on the crystallization of amorphous $\text{Ge}_2\text{Sb}_2\text{Te}_5$. Our goal has been to obtain information about the rapid phase-change mechanism in this material. The refined structure obtained by RMC-DFT/MD simulation for amorphous $\text{Ge}_2\text{Sb}_2\text{Te}_5$ agrees very well with both high-energy x-ray diffraction and x-ray photoelectron spectroscopy data and possesses numerous 4-fold rings comprising *ABAB* alternation (*A*: Ge, Sb; *B*: Te). We propose that they behave as nuclei in the rapid phase-change to the NaCl crystalline phase. A combination of time-resolved x-ray diffraction and photorefectivity measurements has revealed that crystallization of amorphous $\text{Ge}_2\text{Sb}_2\text{Te}_5$ can be

explained by a nucleation-driven process, and we conclude that many such nuclei in a thin amorphous film form the basis of rapid nucleation driven crystallization.

REFERENCES

1. S. R. Ovshinsky: “Reversible electrical switching phenomena in disordered structures”, *Phys. Rev. Lett.* **21** (1968) 1450
2. N. Yamada, E. Ohno, N. Akahira, K. Nishiuchi, K. Nagata and M. Takao: “High speed overwritable phase change disk material”, *Jpn. J. Appl. Phys.* **26**, Suppl. 26–4 (1987) 61
3. H. Iwasaki, Y. Ide, M. Harigaya, Y. Kageyama and I. Fujimura: “Completely erasable phase change optical disk”, *Jpn. J. Appl. Phys.* **31** (1992) 461
4. M. Naito, M. Ishimaru, Y. Hirotsu and M. Takashima: “Local structure analysis of Ge-Sb-Te phase change materials using high-resolution electron microscopy and nanobeam diffraction”, *J. Appl. Phys.* **95** (2004) 8130
5. S. Shamoto, N. Yamada, T. Matsunaga, Th. Proffen, J. W. Richadron, Jr., J.-H. Chung and T. Egami: “Large displacement of germanium atoms in crystalline $\text{Ge}_2\text{Sb}_2\text{Te}_5$ ”, *Appl. Phys. Lett.* **86** (2005) 081904
6. S. Kohara, K. Kato, S. Kimura, H. Tanaka, T. Usuki, K. Suzuya, H. Tanaka, Y. Moritomo, T. Matsunaga, N. Yamada, Y. Tanaka, H. Suematsu and M. Takata: “Structural basis for the fast phase change of $\text{Ge}_2\text{Sb}_2\text{Te}_5$: Ring statistics analogy between the crystal and amorphous states”, *Appl. Phys. Lett.* **89** (2006) 201910
7. P. J  v  ri, I. Kaban, J. Steiner, B. Beuneu, A. Sch  ps and M. A. Webb: “Local order in amorphous $\text{Ge}_2\text{Sb}_2\text{Te}_5$ and GeSb_2Te_4 ”, *Phys. Rev. B* **77** (2007) 035202
8. A. V. Kolobov, P. Fons, A. I. Frenkel, A. L. Ankudinov, J. Tominaga and T. Uruga: “Understanding the phase-change mechanism of rewritable optical media”, *Nature Mater.* **3** (2004) 703
9. D. A. Baker, M. A. Paesler, G. Lucovsky, S. C. Agarwal and P. C. Taylor: “Application of bond constraint theory to the switchable optical memory material $\text{Ge}_2\text{Sb}_2\text{Te}_5$ ”, *Phys. Rev. Lett.* **96** (2006) 255501
10. J. J. Kim, K. Kobayashi, E. Ikenaga, M. Kobata, S. Ueda, T. Matsunaga, K. Kifune, R. Kojima and N. Yamada: “Electronic structure of amorphous and crystalline $(\text{GeTe})_{1-x}(\text{Sb}_2\text{Te}_3)_x$ investigated using hard x-ray photoemission spectroscopy”, *Phys. Rev. B* **76** (2007) 115124
11. W. Welnic, A. Pamungkas, R. Detemple, C. Steimer, S. Bl  gel and M. Wuttig: “Unravelling the interplay of local structure and physical properties in phase-change materials”, *Nature Mater.* **5** (2006) 56
12. S. Caravati, M. Bernasconi, T. D. K  hne, M. Krack and M. Parrinello: “Coexistence of tetrahedral- and octahedral-like sites in amorphous phase change materials”, *Appl. Phys. Lett.* **91** (2007) 171906
13. C. Lang, S. A. Song, D. N. Manh and D. J. H. Cockayne: “Building blocks of amorphous $\text{Ge}_2\text{Sb}_2\text{Te}_5$ ”, *Phys. Rev. B* **76** (2007) 054101
14. J. Akola and R. O. Jones: “Structural phase transitions on the nanoscale: The crucial pattern in the phase-change materials $\text{Ge}_2\text{Sb}_2\text{Te}_5$ and GeTe ”, *Phys. Rev. B* **76** (2007) 235201; J. Akola and R. O. Jones: “Density functional study of amorphous, liquid and crystalline $\text{Ge}_2\text{Sb}_2\text{Te}_5$: homopolar bonds and/or AB alternation?”, *J. Phys.: Condens. Matter* **20** (2008) 465103
15. J. Heged  s and S. R. Elliott: “Microscopic origin of the fast crystallization ability of Ge–Sb–Te phase-change memory materials”, *Nature Mater.* **7** (2008) 399

16. Z. Sun, J. Zhou, A. Blomqvist, B. Johansson and R. Ahuja: "Formation of large voids in the amorphous phase-change memory $\text{Ge}_2\text{Sb}_2\text{Te}_5$ Alloy", *Phys. Rev. Lett.* **102** (2009) 075504
17. J. Wei and F. Gan: "Theoretical explanation of different crystallization processes between as-deposited and melt-quenched amorphous $\text{Ge}_2\text{Sb}_2\text{Te}_5$ thin films", *Thin Solid Films* **441** (2003) 292
18. Y. Fukuyama, N. Yasuda, J. Kim, H. Murayama, Y. Tanaka, S. Kimura, K. Kato, S. Kohara, Y. Moritomo, T. Matsunaga, R. Kojima, N. Yamada, H. Tanaka, T. Ohshima and M. Takata: "Time-resolved investigation of nanosecond crystal growth in rapid-phase-change materials: Correlation with the recording speed of digital versatile disc media", *Appl. Phys. Exp.* **1** (2008) 045001
19. J. Akola, R. O. Jones, S. Kohara, S. Kimura, K. Kobayashi, M. Takata, T. Matsunaga, R. Kojima and N. Yamada: "Experimentally constrained density-functional calculations of the amorphous structure of the prototypical phase-change material $\text{Ge}_2\text{Sb}_2\text{Te}_5$ ", *Phys. Rev. B* **80** (2009) 020201(R)
20. S. Kohara, M. Itou, K. Suzuya, Y. Inamura, Y. Sakurai, Y. Ohishi and M. Takata: "Structural studies of disordered materials using high-energy x-ray diffraction from ambient to extreme conditions", *J. Phys.: Condens. Matter* **19** (2007) 506101
21. S. Kimura, Y. Moritomo, Y. Tanaka, H. Tanaka, K. Toriumi, K. Kato, N. Yasuda, Y. Fukuyama, J. Kim, H. Murayama and M. Takata: "X-ray pinpoint structural measurement for nanomaterials and devices at BL40XU of the SPring-8", *AIP Conf. Proc.* **879** (2007) 1238
22. CPMD V3.12, Copyright IBM Corp 1990–2008, Copyright MPI für Festkörperforschung Stuttgart 1997–2001 (<http://www.cpmd.org>)
23. J. Tao, J. P. Perdew, V. N. Staroverov and G. E. Scuseria: "Climbing the density functional ladder: Nonempirical meta-generalized gradient approximation designed for molecules and solids", *Phys. Rev. Lett.* **91** (2003) 146401
24. O. Gereben, P. Jónvári, L. Temleitner and L. Pusztai: "A new version of the RMC++ Reverse Monte Carlo programme, aimed at investigating the structure of covalent glasses", *J. Optoelectron. Adv. Mater.* **9** (2007) 3021
25. M. T. Dove, M. G. Tucker and D. A. Keen: "Neutron total scattering method: simultaneous determination of long-range and short-range order in disordered materials", *Eur. J. Mineral.* **14** (2002) 331
26. K. Daly Flynn and D. A. Strand: "Crystallization of GeSbTe and AgInSbTe under dynamic conditions", *Proc. SPIE*, **4342** (2002) 94